Radiation Effect on the Mixed Convection Flow of a Viscoelastic Fluid Along an Inclined Stretching Sheet

Muhammad Qasim[a], Tasawar Hayat[b], and Saleem Obaidat[c]

[a] Department of Mathematics, COMSATS Institute of Information Technology (CIIT), Park Road, Chak Shahzad, Islamabad, Pakistan
[b] Department of Mathematics, Quaid-I-Azam University 45320, Islamabad 44000, Pakistan
[c] Department of Mathematics, College of Sciences, King Saud University P.O. Box 2455, Riyadh 11451, Saudi Arabia

Reprint requests to M. Q.; E-mail: mq_qau@yahoo.com

Z. Naturforsch. **67a,** 195 – 202 (2012) / DOI: 10.5560/ZNA.2012-0006
Received June 30, 2011 / revised December 18, 2011

This study concentrates on the heat transfer analysis of the steady flow of viscoelastic fluid along an inclined stretching surface. Analysis has been carried out in the presence of thermal radiation and the Rosseland approximation is used to describe the radiative heat flux in the energy equation. The equations of continuity, momentum and energy are reduced into the system of governing differential equations and solved by homotopy analysis method (HAM). The velocity and temperature are illustrated through graphs. Exact and homotopy solutions are compared in a limiting sense. It is noticed that viscoelastic parameter decreases the velocity and boundary layer thickness. It is also observed that increasing values of viscoelastic parameter reduces the thickness of momentum boundary layer and increase the heat transfer rate. However, it is found that increasing the radiation parameter has the effect of decreasing the local Nusselt number.

Key words: Inclined Stretching; Thermal Radiation; Mixed Convection; Series Solution.

1. Introduction

Recently the heat transfer analysis in boundary layer flow induced by a stretched surface has gained much interest because of its engineering and industrial applications. For instance in the extrusion of plastic sheets, spinning of fibers, polymer, cooling of elastic sheets and many others. The quality of final product strongly depends upon heat transfer rate and thus cooling process can be controlled effectively. Further, the concept of radiative heat transfer in the flow has an important role in manufacturing industries for the design of reliable equipment, nuclear plants, gas turbines and various propulsion devices for aircraft, missiles, satellites and space vehicles. The flow of a viscous fluid over a moving surface was initiated by Sakiadis [1, 2]. Crane [3] derived similarity solution in closed form for the flow of viscous fluid induced by a stretching sheet. At the present there is large number of papers dealing with the flow of viscous and non-Newtonian fluids over a stretching sheet. We have just mentioned some recent representative studies in this direction [4 – 14]. In a very recent study, Haung et al. [15] discussed the heat mass transfer in flow of a viscous fluid along an inclined stretching sheet.

To the best of our knowledge no study has been presented for the heat transfer analysis in the flow of a viscoelastic fluid along an inclined stretching sheet. The object of present work is to address this issue. Hence two-dimensional flow of an incompressible fluid in the presence of thermal radiation has been considered. The flow problem is computed by homotopy analysis method (HAM) [16 – 25]. The variations of embedded parameters on the velocity and temperature are displayed and discussed.

2. Definition of Governing Problem

We consider the steady two-dimensional mixed convection flow of an incompressible viscoelastic fluid over an inclined stretching surface. The heat transfer is considered in the presence of thermal radiation subject to Rosseland approximation. The x-axis is measured along the stretching surface and y-axis normal

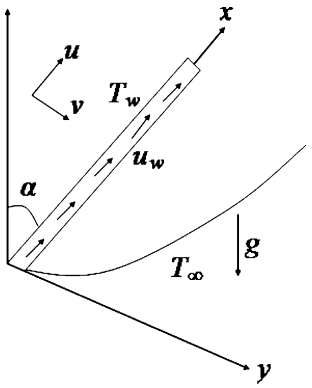

Fig. 1. Physical model and coordinate system.

to the x-axis (Fig. 1). The governing equations through conservation of mass, momentum and energy can be written as

$$\frac{\partial u}{\partial x}+\frac{\partial v}{\partial y}=0, \tag{1}$$

$$u\frac{\partial u}{\partial x}+v\frac{\partial u}{\partial y}=\nu\frac{\partial^2 u}{\partial y^2}-k_0\left[u\frac{\partial^3 u}{\partial x\partial y^2}+\frac{\partial u}{\partial x}\frac{\partial^2 u}{\partial y^2}+\frac{\partial u}{\partial y}\frac{\partial^2 v}{\partial y^2}+v\frac{\partial^3 u}{\partial y^3}\right]+g\beta_{\mathrm{T}}(T-T_\infty)\cos\alpha, \tag{2}$$

$$\rho c_p\left(u\frac{\partial T}{\partial x}+v\frac{\partial T}{\partial y}\right)=\frac{\partial}{\partial y}\left(\left(\frac{16\sigma^* T_\infty^3}{3k^*}+k\right)\frac{\partial T}{\partial y}\right), \tag{3}$$

in which u and v are the velocity components in the x- and y-directions, σ^* is the Stefan–Boltzmann constant, T is the fluid temperature, g is gravitational acceleration, ν is the kinematic viscosity, σ is the electrical conductivity, ρ is fluid density, β_{T} is thermal expansion coefficients of temperature, c_p is specific heat and k^* the mean absorption coefficient.

The boundary conditions relevant to the problem are defined as follows:

$$u=cx,\ \ v=0,\ \ T=T_w,\ \text{at } y=0, \tag{4}$$

$$u\to 0,\ \ T\to T_\infty,\ \text{as } y\to\infty. \tag{5}$$

with surface temperature T_w equal to

$$T_w=T_\infty+bx, \tag{6}$$

where b and c are the positive constants. We define the following variables

$$\eta=\sqrt{\frac{c}{\nu}}y,\ \ \psi=\sqrt{c\nu}xf(\eta),\ \ \theta(\eta)=\frac{T-T_\infty}{T_w-T_\infty}, \tag{7}$$

Introducing the stream function ψ by

$$u=\frac{\partial\psi}{\partial y}\quad v=-\frac{\partial\psi}{\partial x}, \tag{8}$$

the continuity equation is identically satisfied and the resulting problems for f and θ are given by

$$f'''-f'^2+ff''-K[2f'f'''-f''^2-ff'''']+\lambda\theta\cos\alpha=0, \tag{9}$$

$$(1+\mathrm{Nr})\theta''+\mathrm{Pr}(f\theta'-f'\theta)=0, \tag{10}$$

$$f(0)=0,\ \ f'(0)=1,\ \ f'(\infty)\to 0,\ \ \theta(0)=1,\ \ \theta(\infty)\to 0. \tag{11}$$

In the above expressions $K=\dfrac{k_0 c}{\upsilon}$ is the dimensionless fluid parameter, $\lambda=\dfrac{\mathrm{Gr}_x}{\mathrm{Re}_x^2}$ is mixed convection parameter, $\mathrm{Gr}_x\left(=\dfrac{g\beta(T_w-T_\infty)x^3/\upsilon^2}{u_w^2x^2/\upsilon^2}\right)$ is the local Grashof number, $\mathrm{Re}_x=u_w x/\upsilon$ is the local Reynolds number, $\mathrm{Pr}=\dfrac{\mu c_p}{k}$ is the Prandtl number, $\mathrm{Nr}\left(=\dfrac{4\sigma^* T_\infty^3}{k^*k}\right)$ is the radiation parameter and primes indicate the differentiation with respect to η.

The skin friction coefficient C_f and local Nusselt number Nu_x are presented as follows:

$$C_f=\frac{\tau_w}{\rho u_w^2}, \tag{12}$$

$$\mathrm{Nu}=\frac{xq_w}{k(T_w-T_\infty)}, \tag{13}$$

where the skin-friction τ_w and wall heat flux q_w are defined as follows

$$\tau_w=\left[\mu\frac{\partial u}{\partial y}+k_0\left(2\frac{\partial u}{\partial x}\frac{\partial u}{\partial y}+u\frac{\partial^2 u}{\partial x\partial y}+v\frac{\partial^2 u}{\partial y^2}\right)\right]_{y=0}, \tag{14}$$

$$q_w=-k\left(\frac{\partial T}{\partial y}\right)_{y=0}. \tag{15}$$

Substituting (7) and (8) into (14) and (15) we obtain

$$\mathrm{Re}_x^{1/2}C_f=(1+3K)f''(0), \tag{16}$$

$$\mathrm{Re}_x^{1/2}\mathrm{Nu}_x=-\theta'(0), \tag{17}$$

Exact solutions of (9)–(10) for $\lambda = 0$ are

$$f(\eta) = \left[\frac{1-\exp(-A\eta)}{A}\right], \quad K = \frac{1}{\sqrt{1-K}}$$
$$\theta(\eta) = \exp\left(-\frac{\eta}{A}\right)\frac{{}_1\mathrm{F}_1[\frac{B}{A^2};\frac{B}{A^2}-1;-\frac{B}{A^2}\exp(-\eta A)]}{{}_1\mathrm{F}_1[\frac{\mathrm{Pr}}{A^2};\frac{\mathrm{Pr}}{A^2}-1;-\frac{\mathrm{Pr}}{A^2}]},$$
$$B = \frac{\mathrm{Pr}}{1+\mathrm{Nr}}, \tag{18}$$

where ${}_1\mathrm{F}_1$ are the confluent hypergeometric functions.

3. Solution Expressions

In order to find the homotopy solutions, we express f and θ in the set of base functions

$$\{\eta^k \exp(-n\eta) | k \geq 0, n \geq 0\} \tag{19}$$

by the following definitions

$$f(\eta) = a_{0,0}^0 + \sum_{n=0}^{\infty}\sum_{k=0}^{\infty} a_{m,n}^k \eta^k \exp(-n\eta), \tag{20}$$
$$\theta(\eta) = \sum_{n=0}^{\infty}\sum_{k=0}^{\infty} b_{m,n}^k \eta^k \exp(-n\eta), \tag{21}$$

where $a_{m,n}$ and $b_{m,n}$ are the coefficients.

Initial guesses f_0 and θ_0 and auxiliary linear operators are taken as

$$f_0(\eta) = 1-\exp(-\eta), \quad \theta_0(\eta) = \exp(-\eta), \tag{22}$$
$$\mathcal{L}_f = \frac{\mathrm{d}^3 f}{\mathrm{d}\eta^3} - \frac{\mathrm{d}f}{\mathrm{d}\eta}, \mathcal{L}_\theta = \frac{\mathrm{d}^2\theta}{\mathrm{d}\eta^2} - \theta, \tag{23}$$

where

$$\begin{aligned}&\mathcal{L}_f[C_1 + C_2\exp(\eta) + C_3\exp(-\eta)] = 0,\\ &\mathcal{L}_\theta[C_4\exp(\eta) + C_5\exp(-\eta)] = 0,\end{aligned} \tag{24}$$

in which C_i $(i = 1-5)$ are arbitrary. Introducing $p \in [0,1]$ as the embedding parameter and $\hbar_f$ and $\hbar_\theta$ the non-zero auxiliary parameters, the zeroth-order deformation problems are presented as follows:

$$\begin{aligned}&(1-p)\mathcal{L}_f[\hat{f}(\eta,p) - f_0(\eta)]\\ &= p\hbar_f \mathcal{N}_f[\hat{f}(\eta,p), \hat{\theta}(\eta,p)],\end{aligned} \tag{25}$$
$$\begin{aligned}&(1-p)\mathcal{L}_\theta[\hat{\theta}(\eta,p) - \theta_0(\eta)]\\ &= p\hbar_\theta \mathcal{N}_\theta[\hat{f}(\eta,p), \hat{\theta}(\eta,p)],\end{aligned} \tag{26}$$
$$\begin{aligned}&\hat{f}(\eta;p)\big|_{\eta=0} = 0, \quad \left.\frac{\partial \hat{f}(\eta;p)}{\partial\eta}\right|_{\eta=0} = 1,\\ &\left.\frac{\partial \hat{f}(\eta;p)}{\partial\eta}\right|_{\eta=\infty} = 0,\end{aligned} \tag{27}$$
$$\hat{\theta}(\eta;p)\big|_{\eta=0} = 1, \quad \hat{\theta}(\eta;p)\big|_{\eta=\infty} = 0, \tag{28}$$
$$\begin{aligned}\mathcal{N}_f[\hat{f}(\eta;p), \hat{\theta}(\eta;p)] &= \frac{\partial^3 \widehat{f}(\eta;p)}{\partial\eta^3} - \left(\frac{\partial \widehat{f}(\eta;p)}{\partial\eta}\right)^2\\ &+ \widehat{f}(\eta;p)\frac{\partial^2 \widehat{f}(\eta;p)}{\partial\eta^2} + \lambda\cos\alpha\hat{\theta}(\eta,p)\\ &- K\left[+2\frac{\partial \widehat{f}(\eta;p)}{\partial\eta}\frac{\partial^3 \widehat{f}(\eta;p)}{\partial\eta^3}\right.\\ &\left.- \frac{\partial \widehat{f}(\eta;p)}{\partial\eta}\frac{\partial^4 \widehat{f}(\eta;p)}{\partial\eta^4} - \left(\frac{\partial^2 \widehat{f}(\eta;p)}{\partial\eta^2}\right)^2\right],\end{aligned} \tag{29}$$
$$\begin{aligned}\mathcal{N}_\theta[\hat{f}(\eta;p), \hat{\theta}(\eta;p)] &= \left(1+\frac{4}{3}\mathrm{Nr}\right)\frac{\partial^2\hat{\theta}(\eta,p)}{\partial\eta^2}\\ &+ \mathrm{Pr}\left(\widehat{f}(\eta;p)\frac{\partial\widehat{\theta}(\eta;p)}{\partial\eta} - \widehat{\theta}(\eta;p)\frac{\partial\widehat{f}(\eta;p)}{\partial\eta}\right)\end{aligned} \tag{30}$$

Substituting $p = 0$ and $p = 1$, we have

$$\widehat{f}(\eta;0) = f_0(\eta), \quad \widehat{f}(\eta;1) = f(\eta), \tag{31}$$
$$\widehat{\theta}(\eta;0) = \theta_0(\eta), \quad \widehat{\theta}(\eta;1) = \theta(\eta) \tag{32}$$

and when p increases from 0 to 1, $\widehat{f}(\eta;p)$ and $\widehat{\theta}(\eta;p)$ deforms from $f_0(\eta)$ and $\theta_0(\eta)$ to $f(\eta)$ and $\theta(\eta)$ respectively. Further Taylors' series expansion results

$$\widehat{f}(\eta;p) = f_0(\eta) + \sum_{m=1}^{\infty} f_m(\eta)p^m, \tag{33}$$
$$\widehat{\theta}(\eta;p) = \theta_0(\eta) + \sum_{m=1}^{\infty} \theta_m(\eta)p^m, \tag{34}$$
$$\begin{aligned}f_m(\eta) &= \left.\frac{1}{m!}\frac{\partial^m \widehat{f}(\eta;p)}{\partial p^m}\right|_{p=0},\\ \theta_m(\eta) &= \left.\frac{1}{m!}\frac{\partial^m \widehat{\theta}(\eta;p)}{\partial p^m}\right|_{p=0},\end{aligned} \tag{35}$$

and the auxiliary parameters $\hbar_f$ and $\hbar_\theta$ are selected in such a manner that the series (20) and (21) converge at $p = 1$. Hence

$$\begin{aligned}f(\eta) &= f_0(\eta) + \sum_{m=1}^{\infty} f_m(\eta),\\ \theta(\eta) &= \theta_0(\eta) + \sum_{m=1}^{\infty} \theta_m(\eta),\end{aligned} \tag{36}$$

and the associated problem at mth order are

$$\begin{aligned}&\mathcal{L}_f[f_m(\eta) - \chi_m f_{m-1}(\eta)] = \hbar_f \mathcal{R}_m^f(\eta),\\ &\mathcal{L}_\theta[\theta_m(\eta) - \chi_m \theta_{m-1}(\eta)] = \hbar_\theta \mathcal{R}_m^\theta(\eta),\end{aligned} \tag{37}$$

$$f_m(0)=0, f'_m(0)=0, f'_m(\infty)=0,$$
$$\theta_m(0)=0, \theta_m(\infty)=0, \phi_m(0)=0, \phi_m(\infty)=0, \quad (38)$$

$$\mathcal{R}^f_m(\eta)=f'''_{m-1} + \sum_{k=0}^{m-1}\begin{pmatrix} f_{m-1-k}f''_k - f'_{m-1-k}f'_k \\ -K\left(2f_{m-1-k}f'''_k - f''_{m-1-k}f''_k - f_{m-1-k}f''''_k\right)\end{pmatrix} + \lambda\cos a\,\theta_{m-1-k}, \quad (39)$$

$$\mathcal{R}^\theta_m(\eta)=\left(1+\frac{4}{3}\mathrm{Nr}\right)\theta''_{m-1} + \mathrm{Pr}\sum_{k=0}^{m-1}\left(f_{m-1-k}\theta'_k - f'_{m-1-k}\theta_k\right), \quad (40)$$

$$\chi_m=\begin{cases}0, & m\le 1\\ 1, & m>1\end{cases}. \quad (41)$$

The general solutions of (39)–(41) are obtained as follows:

$$f_m(\eta)=f^*_m(\eta)+C_1+C_2\exp(\eta)+C_3\exp(-\eta), \quad (42)$$
$$\theta_m(\eta)=\theta^*_m(\eta)+C_4\exp(\eta)+C_5\exp(-\eta), \quad (43)$$

where $f^*_m(\eta)$ and $\theta^*_m(\eta)$ are the special solutions and

$$C_2=C_4=0,$$
$$C_1=-C_3-f^*_m(0),\ C_3=\left.\frac{\partial f^*_m(\eta)}{\partial\eta}\right|_{\eta=0}, \quad (44)$$
$$C_5=-\theta^*_m(0).$$

4. Convergence of the Series Solutions

Clearly the non-zero auxiliary parameters $\hbar_f$ and $\hbar_\theta$ are present in the solutions (33) and (34). These parameters have indispensable role in controlling and adjusting the permissible range of convergence, the $\hbar_f$ and $\hbar_\theta$ curves are presented for 20th-order of approximation. The admissible values of $\hbar_f$ and $\hbar_\theta$ are $-1.1\le\hbar_f$, $\hbar_\theta\le-0.3$ (Fig. 2). The series given by (36) converge in the whole region of η when $\hbar_f=\hbar_\theta=-0.6$. Table 1 indicates the convergence of the homotopy analysis solutions for different order of approximations.

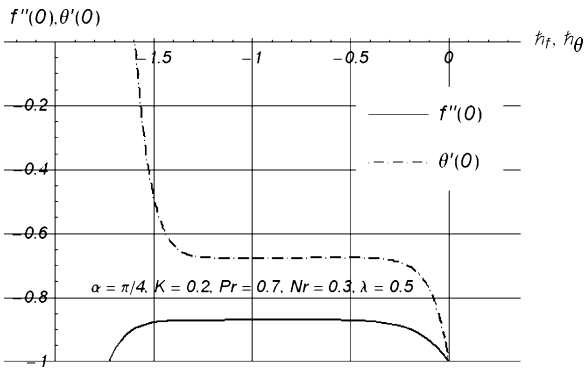

Fig. 2. $\hbar$-curves of the functions $f''(0)$ and $\theta'(0)$ at 20th order of approximation.

Table 1. Convergence of homotopy solutions for different order of approximations when $\alpha=\pi/4$, $K=0.2$, $\lambda=1.0$, $\mathrm{Pr}=1.0$ and $\mathrm{Nr}=0.3$.

Order of approximation	$-f''(0)$	$-\theta'(0)$
0	0.82251	0.85177
10	0.67463	0.87595
20	0.67339	0.87605
30	0.67334	0.87603
35	0.67334	0.87602
40	0.67334	0.8760

5. Results and Discussion

The object of this section is to examine the velocity and concentration for various parameters of interest. A comparative study between exact and the homotopy solution for the velocity $f'(\eta)$ and the concentration field field $\theta(\eta)$ is presented in the Figures 3 and 4 when $\lambda=0$. These figures show an excellent agreement between the exact solution and homotopy solution at 15th-order of approximations. The variations of K, λ, α, Pr and Nr have been sketched in Figures 5–9. Figure 5 depicts the velocity profile $f'(\eta)$ and temperature θ for various values of viscoelastic parameter K. It is found that velocity $f'(\eta)$ decreases as the viscoelastic parameter increases (Fig. 5a) but temperature increases in this case (Fig. 5b). Figure 6 plots the effects of mixed convection parameters λ on the velocity and temperature profiles. The influence of buoyancy parameter λ decreases the thermal boundary layer. Increasing buoyancy parameter corresponds to the stronger buoyancy force and thus lead to the larger velocity. The larger velocity accompanies with decreasing boundary layer thickness for temperature. It is interesting to observe that for large inclination α the boundary layer thickness increases (Fig. 7a) whereas opposite effects are found in case of temperature distribution Figure 8. Infact increasing values of λ corresponds to the stronger buoyancy force which causes an

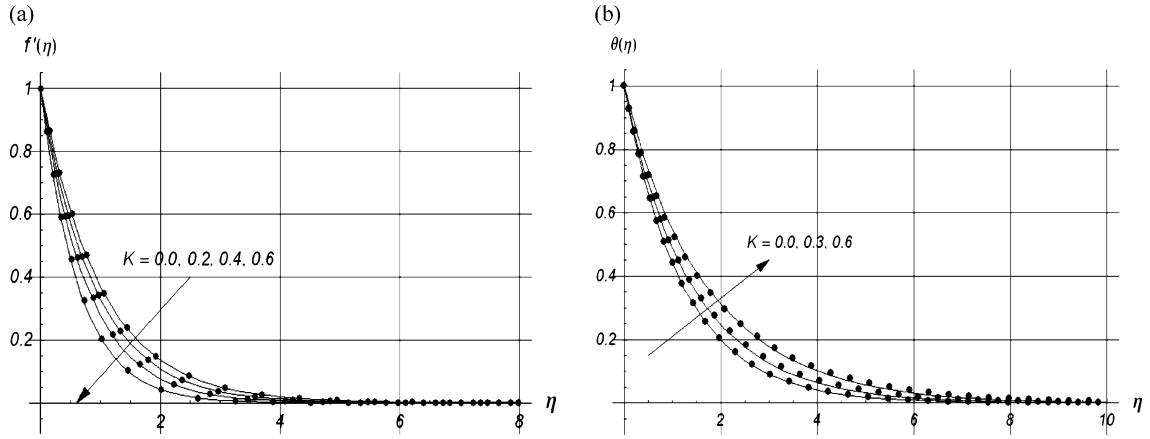

Fig. 3. Comparison of $f'(\eta)$ for the analytical approximation with an exact solution when $\lambda = 0$. Filled circle: exact solution; solid line: 15th-order HAM solution.

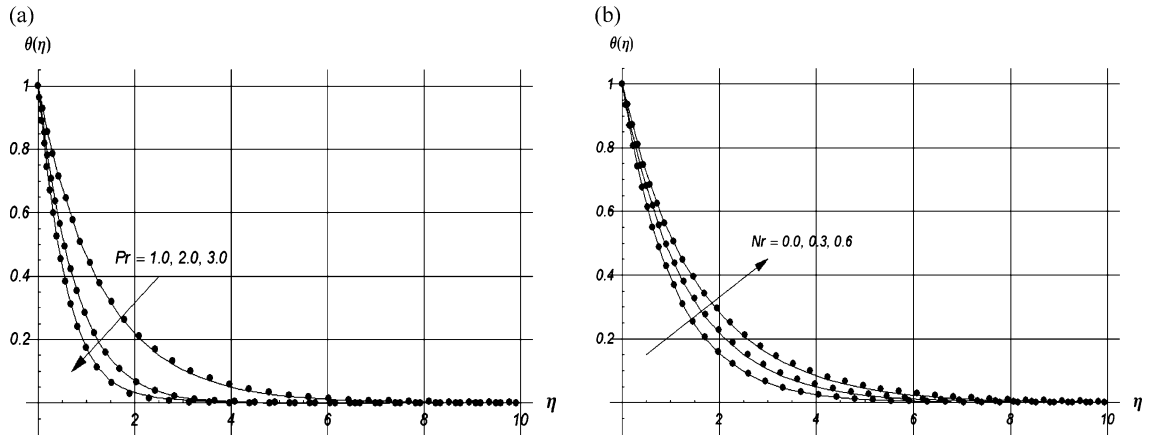

Fig. 4. Comparison of $\theta(\eta)$ for the analytical approximation with the numerical solutions when $\lambda = 0$. Filled circle: numerical solution; solid line: 15th-order HAM solution.

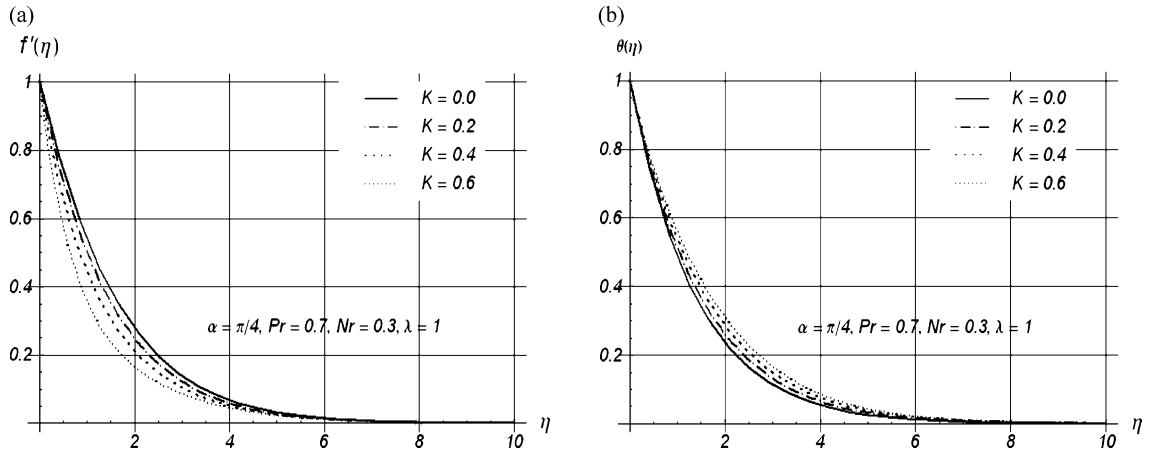

Fig. 5. Influence of viscoelastic parameter K on f' and θ.

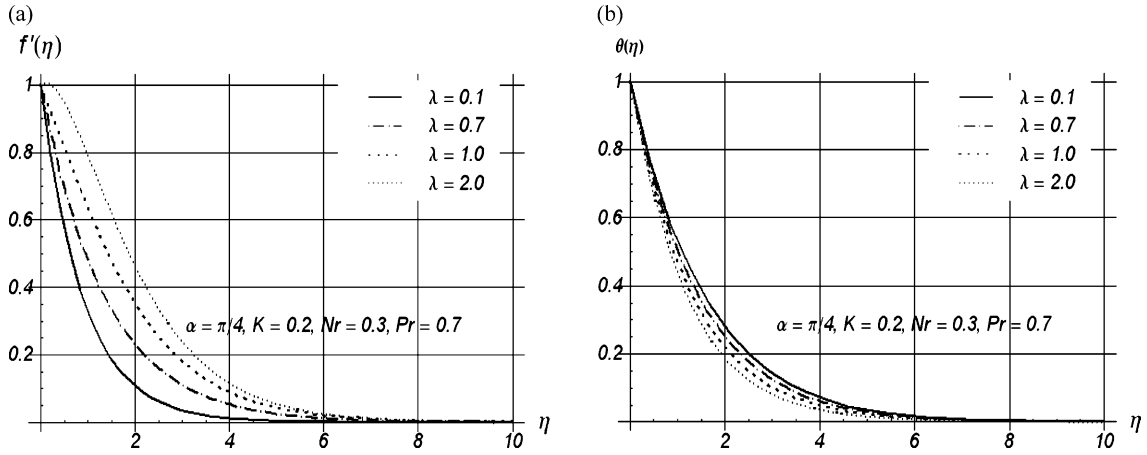

Fig. 6. Influence of mixed convection parameter λ on f' and θ.

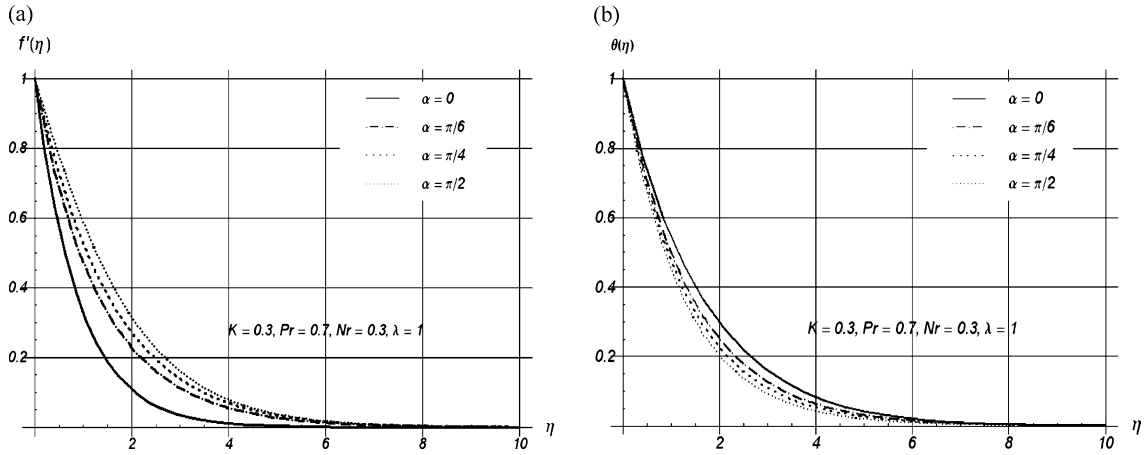

Fig. 7. Influence of sheet inclination α on f' and θ.

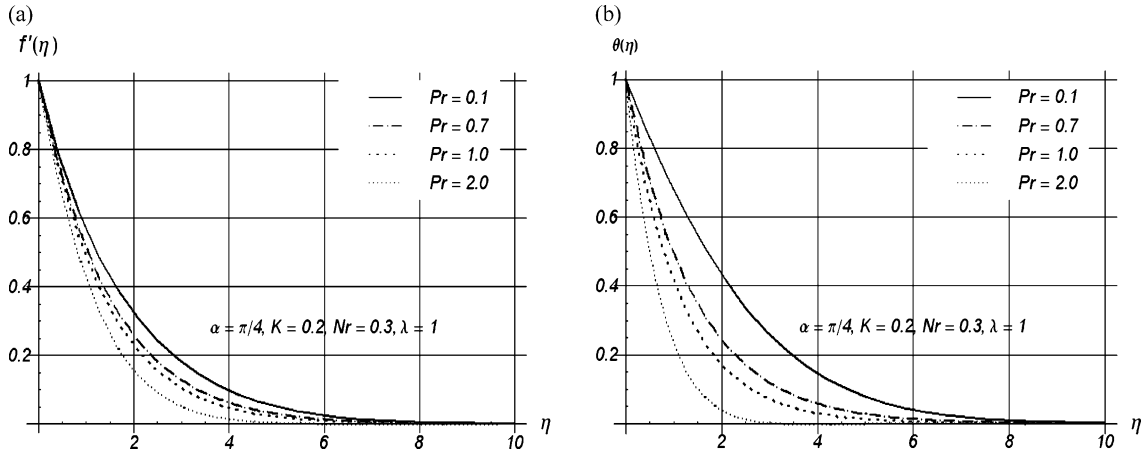

Fig. 8. Influence of Prandtl number Pr on f' and θ.

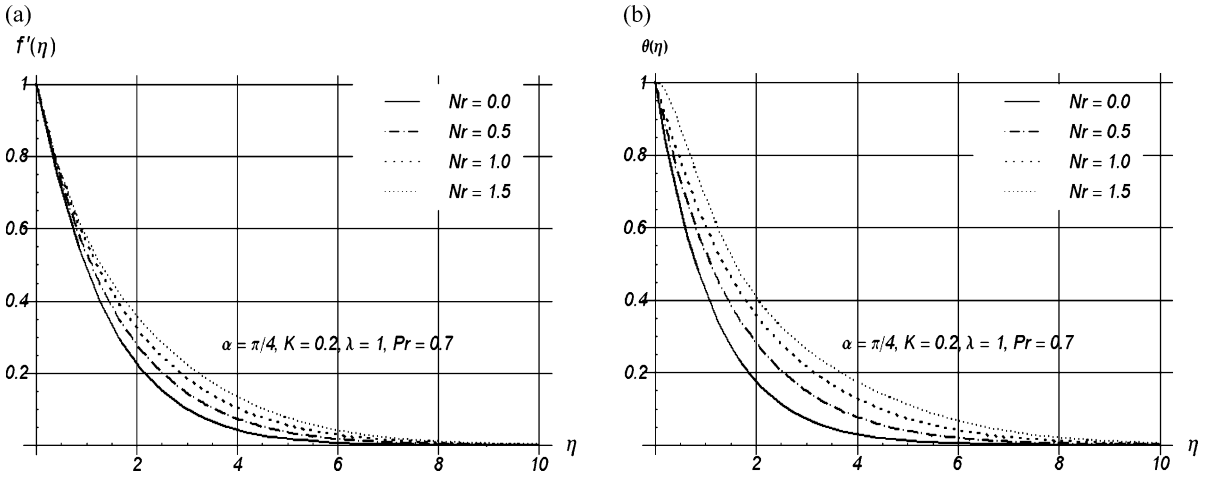

Fig. 9. Influence of radiation parameter Nr on f' and θ.

Table 2. Local Nusselt number $\mathrm{Re}_x^{-1/2}\mathrm{Nu}_x$ for some values of λ, Pr, K, and Nr when $\alpha = \pi/4$.

λ	K	Pr	Nr	$-\mathrm{Re}_x^{-1/2}\,\mathrm{Nu}_x$
0.0	1.0	1.0	0.3	0.77372
1.0				0.87565
2.0				0.93747
1.5	0.0	1.0	0.3	0.90985
	0.2			0.90926
	0.4			0.90912
1.2	0.1	0.5	0.3	0.61227
		0.7		0.73526
		1.2		0.98682
1.5	0.1	0.7	0.0	0.88224
			0.5	0.66862
			1.0	0.55747

increase in flow velocity. Figure 8 illustrates the effects of Prandtl number on the velocity and temperature profiles. It is observed that the effects of the Prandtl number decreases both velocity and thermal boundary layer thickness. Infact an increase in the Prandtl number leads to an increase in fluid viscosity which causes a decrease in the flow velocity. Note that $\mathrm{Pr} < 1$ corresponds to the flows for which momentum diffusivity is less than the thermal diffusivity. An increase in the weaker thermal diffusivity therefore results in thinning the thermal boundary layer. Note that Figure 9 represent the variations of velocity and temperature profiles for various values of the radiation parameter Nr. Figure 9a depicts that velocity increases with the increase of radiation parameter Nr. It is found that an increase in Nr significantly increases the temperature θ (Fig. 9b). Thus radiation should be minimized to have the cooling process at a faster rate. Numerical values of local Nusselt number for various values of embedding parameters are computed in Table 2. It is noticed that local Nusselt number is an increasing function of λ and Pr. However an increase in Nr causes a reduction in the magnitude of local Nusselt number.

6. Concluding Remarks

In this work, the effect of thermal radiation on the mixed convection boundary layer flow and heat transfer in a viscoelastic fluid over an inclined stretching sheet is studied. The main observations are presented as follows.

- The HAM solutions for velocity and temperature fields are in an excellent agreement with the exact solution.
- The effect of viscoelastic parameter K on velocity and thermal boundary layer thickness are quite opposite.
- An increase in the viscoelastic parameter K results a decrease in the velocity and the associated boundary layer thickness. However the temperature and the thermal boundary layer thickness increase when K increases.

- An increase in Prandtl number Pr reduces the temperature and the thermal boundary layer thickness.
- The values for Nusselt number for viscoelastic fluid are more than the viscous fluid.

Acknowledgement

Second author as a visiting Professor thanks the King Saud University for the support (KSU-VPP-117).

[1] B. C. Sakiadis, AICHE J. **7**, 26 (1961).
[2] B. C. Sakiadis, AICHE J. **7**, 221 (1961).
[3] L. J. Crane, ZAMP **21**, 645 (1970).
[4] R. Cortell, Comput. Math. Appl. **53**, 305 (2007).
[5] R. Cortell, Int. J. Nonlin. Mech. **41**, 78 (2006).
[6] H. Xu and S. J. Liao, Comput. Math. Appl. **57**, 1425 (2009).
[7] T. Hayat, M. Qasim, and Z. Abbas, Int. J. Numer. Meth. Fluids **66**, 194 (2011).
[8] R. Cortell, Chem. Eng. Process. **46**, 982 (2007).
[9] T. Hayat and M. Qasim, Int. J. Heat Mass Transfer **53**, 4780 (2010).
[10] S. Mukhopadhyay, Nucl. Eng. Des. **241**, 2660 (2011).
[11] T. Hayat, M. Awais, M. Qasim, and A. Hendi, Int. J. Heat Mass Transfer **54**, 3777 (2011).
[12] S. Mukhopadhyay, Int. J. Heat Mass Transfer **52**, 3261 (2009).
[13] T. Hayat, M. Qasim, Z. Abbas, and A. A. Hendi, Z. Naturforsch. **64a**, 1111 (2010).
[14] T. Hayat, M. Qasim, and Z. Abbas, Z. Naturforsch **65a**, 231 (2010).
[15] J. S. Huang, R. Tsai K. H. Haung, and C. H. Huang, Chem. Eng. Commun. **198**, 453 (2011).
[16] S. J. Liao, Beyond perturbation: Introduction to homotopy analysis method, Chapman and Hall, CRC Press, Boca Reton 2003.
[17] N. Kousar and S. J. Liao, Transport Porous Med. **83**, 397 (2010).
[18] S. Abbasbandy, Chaos Solitons Fract. **39**, 428 (2009).
[19] S. Abbasbandy and E. Shivanian, Commun. Nonlin. Sci. Numer. Simul. **16**, 112 (2011).
[20] T. Hayat, M. Qasim, and Z. Abbas, Commun. Nonlin. Sci. Numer. Simul. **15**, 2375 (2010).
[21] I. Hashim, O. Abdulaziz, and S. Momani, Commun. Nonlin. Sci. Numer. Simul. **14**, 674 (2009).
[22] A. S. Bataineh, M. S. M. Noorani, and I. Hashim, Commun. Nonlin. Sci. Numer. Simul. **14**, 409 (2009).
[23] M. Dehghan and R. Salehi, Z. Naturforsch. **66a**, 259 (2011).
[24] T. Hayat and M. Qasim, Z. Naturforsch. **65**, 950 (2010).
[25] T. Hayat, S. A. Shehzad, and M. Qasim, Z. Naturforsch. **66a**, 417 (2011).